Colorectal tumor-induced orexigenic imbalance lowers protein appetite and drives early organ wasting symptoms

Afroditi Petsakou[1]*, Elizabeth Filine[1], Matthew Li[1], Alice Zheng[1], and Norbert Perrimon[1,2]*

[1]*Department of Genetics, Harvard Medical School, Boston, USA*
[2]*Howard Hughes Medical Institute, Boston, USA*

* Corresponding authors
Afroditi Petsakou: Afroditi_Petsakou@hms.harvard.edu
Norbert Perrimon: perrimon@genetics.med.harvard.edu

Cancer cachexia (CC) is a deadly syndrome characterized by weight loss and wasting of muscle and adipose tissue[1]. Early symptoms include behavioral changes such as anorexia (loss of appetite) that precede weight loss and organ wasting[2]. Around ~50-80% of patients with advanced cancer develop CC[3], generating a pressing need to understand CC progression. Although recent advances have identified distinct metabolic, inflammatory, and neuronal networks associated with CC, the underlying mechanisms initiating early-stage CC remain unclear[1]. This outstanding question has proven difficult to answer in murine models due to the complexity and onset variability of CC. To address this, we utilized a fly colorectal-tumor model with a defined time-window for organ wasting[4]. We discovered that combined increase of conserved factors involved in inflammation (Upd3/Interleukin-6-like) and in reduced insulin signaling (ImpL2/Insulin Growth Factor Binding Protein) cause orexigenic dysfunction prior to organ wasting due to silencing of NPF (Neuropeptide F/ Neuropeptide Y) signaling in the brain. This initiates inadequate protein-specific nutritional choices and anorexia, promoting weight loss. Altogether, we provide evidence for an intricate mechanism that alters protein appetite and drives early organ wasting symptoms.

Activation of the Yorkie (Yki)/Yap oncogene in intestinal progenitor cells (using the *escargot-Gal4* driver, together with the temperature-sensitive Gal4 repressor *Tubulin-Gal80^{TS}*, referred as *esg^{TS}>yki^{act}*) has emerged as an attractive adult-specific colorectal organ wasting model[4-6]. In this model, flies are reared until adulthood in low temperatures (18°C) to inhibit oncogene activation and then temperature is raised to 29°C (defined as day 0, d0) to allow colorectal Yki-tumor induction[4]. A week of Yki-tumor induction leads to the onset of organ

wasting symptoms such as metabolic imbalance (increased lipolysis, reduced insulin signaling), bloating (ascites-like symptom) and reproductive organ atrophy, followed by fat cell degeneration and myofiber degradation[4,7], reminiscent of colorectal CC symptoms. We reasoned that the short and well-defined time window prior to the onset of organ wasting makes this tumor model ideal for identifying early mechanisms linked to organ wasting initiation.

Previously, using a capillary-based assay it was observed that *esg*^{TS}>*yki*^{act} flies had only a subtle decrease in food intake by d6 of tumor growth[4]. Since anorexia is an early symptom of CC, we reexamined food intake in *esg*^{TS}>*yki*^{act} flies using a more sensitive approach. Specifically, we used an automated behavior apparatus (Flypad, Fly Proboscis and Activity Detector) that monitors in real time how long individual flies contact the food[8]. The duration of food contact (total duration of activity bouts) significantly correlates with food ingestion and is used to quantify feeding behavior[8]. Using the Flypad, we observed a significant reduction in the feeding behavior of individual male and female *esg*^{TS}>*yki*^{act} flies (Fig. 1a). As the *escargot-Gal4* driver is expressed subtly in the brain (Fig. 1b) in addition to the gut, which could complicate the interpretation of the results, we co-expressed the neuronal inhibitor *elavGal80* to prevent oncogene activation in the brain (Fig 1b-c). Flies with *yki*^{act} oncogene expression specific to the gut and not the brain (*elavGal80;esg*^{TS}>*yki*^{act} - hereafter referred as Yki^{act}), maintained significantly reduced feeding behavior (Fig 1d), indicating that anorexia-like behavior is due to colorectal tumor growth.

To further verify that food intake in Yki^{act} flies is significantly decreased, we used a dye-based feeding assay, in which a non-toxic non-absorbed blue dye is added to the food, and food consumption is measured by eye-scoring (Fig.1e) or by color spectrophotometry of homogenized flies (Fig. 1f). Indeed, both male and female Yki^{act} flies showed reduce food intake on d6 of gut tumor growth (Fig. 1e-f). In addition, we used this assay to test food intake in flies with colorectal tumors that do not cause organ wasting, such as tumor induction due to activation of the Raf oncogene (*elavGal80;esg*^{TS}>*Raf*^{GOF}) or reduction of the *APC* tumor suppressor (*elavGal80;esg*^{TS}>*APC*^{RNAi}). Food intake was not, or only subtly, affected compared to control (Ext. Data Fig. 1a-b), indicating that the anorexic behavior exhibited by Yki^{act} flies correlates with organ wasting. Finally, we tested whether reduced food intake in Yki^{act} flies is impacted by an alternate diet or the microbiome by changing the food recipe or adding antibiotics, respectively. Neither condition prevented Yki^{act} flies from consuming significantly less food (Ext. Data Fig. 1c-f).

In Yki^{act} flies, metabolic imbalance such as increased lipolysis, which is marked by a significant drop in triglycerides, starts on d6 of tumor induction in both male and female flies

(Ext. Data Fig. 1g). Similarly, when we assayed the dry weight as an indicator of tissue atrophy, we observed a significant reduction after d6 in the dry weight of both male and female Yki^{act} flies (Fig. 1g). Strikingly, we observed that in both male and female Yki^{act} flies the onset of reduced food intake starts on d5 of gut tumor growth (Fig. 1h-i), one day before organ wasting symptoms. Together, these data suggest that in Yki^{act} flies the anorexic behavior precedes organ wasting, reminiscent of CC-related anorexia[2].

We reasoned that if the anorexia in Yki^{act} flies is linked to organ wasting, then tumor-derived secreted factors should be responsible for the changes in feeding behavior. Two of the most highly expressed secreted factors in Yki^{act} flies are the conserved inflammatory cytokine Upd3 and the insulin antagonist ImpL2[4,5], whose mammalian counterparts, IL-6 and IGFBP, respectively, are also associated with CC[1,9-12]. Tumor-derived Upd3 is required for tumor growth[5] and has been reported to disrupt the blood brain barrier[13]. ImpL2 is not required for tumor growth but drives organ wasting symptoms and reduced insulin signaling[4,14]. In addition, insulin and Upd-related signaling are part of the satiety-promoting network in *Drosophila* that stops feeding and represses orexigenic signaling such as Neuropeptide F (NPF)[15-18]. We observed that in Yki^{act} male flies both *upd3* and *ImpL2* expression levels are significantly increased by d4 (Fig. 2a) and in females by d5 (Fig. 2b). Since the elevated expression of *upd3* and *ImpL2* matches the advent of reduced food intake in both male and female Yki^{act} flies, we next asked whether an excess of these factors could promote anorexic behavior independently of colorectal tumor growth. To address this, we conditionally overexpressed *ImpL2* and *upd3* from muscle using the *mef2-Gal4* driver together with the *Tubulin*-Gal80^{TS} repressor (referred as *mef2^{TS}*). Individual overexpression of *ImpL2* or *upd3* (*mef2^{TS}>upd3*, *mef2^{TS}>ImpL2*) for 4 days did not reduce food intake (Fig 2c-d). However, the combined conditional overexpression of *upd3* and *ImpL2* (*mef2^{TS}>upd3+ImpL2*) was sufficient to significantly decrease food intake in both males and females (Fig 2c-d), phenocopying the anorexic behavior of Yki^{act} flies. Altogether, these data support the idea that the combined increase in ImpL2 and Upd3 during colorectal Yki-tumor growth drives anorexia prior to organ wasting.

In recent years *Drosophila* has emerged as a powerful system to study feeding-related mechanisms[17]. Several conserved hunger and satiety signals have been identified[17], as well as mating- and sex-specific mechanisms that differentially regulate feeding behavior in male versus female flies[19-23]. Thus, we sought to identify the feeding pathways that are impacted by Upd3 and ImpL2 in Yki^{act} flies. However, when we tested for changes in the expression of feeding -related signals, we observed distinct changes in male versus female Yki^{act} flies. For example, we detected a significant increase of *upd2/leptin*[18] expression only in females and not males

(Ext. Data Fig. 2a, Fig. 3a), suggesting that feeding behavior is regulated by sex-specific mechanisms even under tumor conditions. Given that feeding-related networks in females are complex due to post-mating sex peptide signaling and egg production[19,21,24,25], we focused on the anorexic behavior of male Yki^{act} flies.

At the onset of anorexia (d5) two feeding-related peptides were significantly decreased in male Yki^{act} flies (Fig. 3a). One peptide is *CCHamide-2* (*ccha2*), which has no known mammalian counterpart and has been proposed to act as a nutrient-stimulated satiety indicator[17], albeit there are conflicting reports regarding its functions[26-28]. Since low expression of *ccha2* has been linked to starvation conditions[26], it is likely that the decrease we observed in Yki^{act} male flies marks the internal nutritional scarcity experienced by d5 due to reduced food intake. The other hunger-related peptide is *NPF*, a homolog of mammalian orexigenic hormone Neuropeptide Y (NPY), which is expressed in enteroendocrine cells in the fly gut and in ~30 neurons in the fly brain[29]. NPF signaling from the gut has distinct roles in male and female flies[21,30]. In males, gut-NPF increases sugar intake upon starvation, whereas in females, gut-NPF inhibits sugar while increasing protein intake[21,30]. In contrast, NPF derived from the brain promotes feeding upon starvation in both males and females[31-33]; and NPF neurons play a vital role in feeding behavior because they integrate different information about the nutritional state of the animal[15,34-36]. Moreover, *NPF* decrease in the brain has been observed previously in an anorexia-organ wasting model caused by tumor growth in the eyes of the fly[37]. However, the role of NPF signaling in tumor-induced anorexia and organ wasting in flies was not explored[37]. In addition, in that study, eye-tumor derived anorexia was also associated with a decrease in the orexigenic *sNPF* (*short Neuropeptide F*) and an increase in the anorexigenic *nucleobinding1* (*nucb1*)[37]. *sNPF* and *nucb1* expression showed no difference in Yki^{act} flies when compared to control (Ext. Data Fig 2a, Fig. 3a), indicating that feeding behavior is regulated by distinct mechanisms in different tumor models. Interestingly, *NPY* reduction is observed in cancer anorexia patients and murine models[37-41]; however, its role in CC remains to be determined. Altogether these prompted us to explore the role of NPF signaling in Yki^{act}.

The decrease in *NPF* levels in Yki^{act} males starts on d4 (Fig. 3b), indicating that it is likely a very early inducer of anorexia and subsequent organ wasting. The start of *NPF* decrease on d4 coincides with the onset of elevated *upd3* and *ImpL2* expression (Fig. 2a), suggesting that these events are linked. Supporting this, anorexic *mef2^{TS}>upd3+ImpL2* male flies exhibit significant *NPF* reduction on d4 (Fig. 3c), equivalent to the one observed in Yki^{act} flies. Therefore, we tested the impact of increased NPF signaling in Yki^{act} male flies. Specifically, we co-expressed the heat-activated thermosensitive cation channel TrpA1 in all NPF-

expressing cells using the *LexAop-TrpA1* transgene together with the *NPFLexA* driver (*elavGal80;esg^{TS}>yki^{act} + NPFLexA>LexAopTrpA1)*. This causes NPF signaling to be increased concurrently with gut-tumor induction when the temperature is raised to 29°C. Notably, elevated NPF signaling was sufficient to rescue anorexia in Yki^{act} male flies on d5 and d6 (Fig 3d-e).

Further, we speculated that this rescue comes from the brain since *NPF* is significantly reduced in the brain in Yki^{act} males (Fig. 3f), whereas *NPF* expression in the gut is variable (Fig. 3f). To test this hypothesis, we assayed feeding behavior while increasing NPF signaling only from the gut. To prevent activation of NPF neurons in Yki^{act} flies, we used the *NPFLexA:GAD* driver that is repressed by the neuronal inhibitor elavGal80 (*elavGal80;esg^{TS}>yki^{act} + NPFLexA:GAD>LexAopTrpA1)*. NPF activation solely from the gut prevented the rescue of the anorexic behavior in Yki^{act} male flies (Fig. 4g), suggesting that neuronal NPF signaling is required for the Yki-induced anorexic phenotypes.

To further test how tumor-derived secreted factors impact NPF neurons, we used an *ex vivo* brain assay (Ext. Data Fig. 2b). Specifically, we expressed the genetically encoded Ca^{2+} indicator GCAMP7b with the *NPFGal4* driver (*NPF>GCAMP7b*) to image the activity of NPF neurons in control brains while adding hemolymph from control or Yki^{act} male flies (Ext. Data Fig. 2b). We focused on the dorsal median P1 NPF neurons (Ext. Data Fig. 2c) as they have been proposed to be indicators of internal state imbalance[36] and are selectively activated by both hunger and food-odor attractiveness[34]. Interestingly, adding control hemolymph in NPF-P1 neurons caused a post-inhibitory excitation response, supporting that hemolymph factors allow neuronal activation (Fig. 3h, Ext. Data Fig. 2d). In contrast, when we added Yki^{act} hemolymph, neuronal responses were repressed, suggesting that tumor-derived secreted factors prevent the activation of NPF-P1 neurons. Furthermore, post-inhibitory excitation of NPF-P1 neurons was inhibited when we added hemolymph from the anorexic male *mef2^{TS} >upd3 + ImpL2* flies (Fig. 3i, Ext. Data Fig. 2e). Taken together, our data support that the combined increase of Upd3 and ImpL2 causes anorexia by repressing NPF signaling in the brain, making Yki^{act} flies non-responsive to internal nutritional needs prior to organ wasting.

We next tested whether NPF dysfunction contributes to tumor growth and organ wasting. Increase of NPF signaling in Yki^{act} male flies did not impact intestinal tumors (Fig. 4a) and did not rescue the reduction in triglycerides that Yki^{act} flies experience on d6 (Ext. Data Fig. 3a). However, NPF activation rescued the decrease in dry weight (Fig. 4b). In addition, NPF activation only from the gut did not rescue the reduction in dry weight (Ext. Data Fig. 3b), suggesting that dry weight loss in Yki^{act} male flies results from neuronal NPF-induced anorexia. Further supporting that anorexia is linked to weight loss, anorexic *mef2^{TS} >upd3 + ImpL2* males

exhibited significant reduction in dry weight (Fig. 4c). Altogether, our data support the model that the combined early increase in Upd3 and ImpL2 results in neuronal NPF dysfunction, and that the resulting anorexic behavior promotes weight loss in Yki^{act} male flies.

Interestingly, when we tested food rich for different macronutrients, we found that Yki^{act} male flies on d6 exhibit anorexic behavior specifically for yeast (protein-rich food), whereas food intake for sugar-rich or fat-rich food was similar to control (Fig. 4d). Protein malnutrition and subsequent internal amino acid (AA) scarcity exacerbates breakdown of tissue protein in CC patients[42,43]. We therefore asked whether reduced intake for yeast in Yki^{act} male flies is specific to AAs and observed that intake for essential AA-rich food is significantly reduced while ingestion of non-essential AA-rich food is the same in Yki^{act} male flies and control (Fig. 4d). Moreover, anorexic male *mef2^{TS} >upd3 + ImpL2* flies consume significantly less protein-rich and essential AA-rich food while sugar intake remains similar to control (Ext. Data Fig. 3c). Together, these data support that in Yki^{act} male flies the combined increase of Upd3 and ImpL2 leads to anorexia for protein-rich food, making them prone to protein-malnutrition.

Nutrient-specific appetite drives selection of foods with specific macronutrients so that nutritional homeostasis and optimal fitness is maintained - a behavior conserved among animals including flies[44-46]. CC patients regularly experience appetite changes, including difficulty ingesting protein-rich foods like meat[47]. Given that a comprehensive understanding of macronutrient preferences in CC patients is lacking[48], it remains unclear whether early changes in nutrient-specific appetites of patients could account for the advent of early-stage CC symptoms. In Yki^{act} male flies, high levels of Upd3 and ImpL2 and the ensuing reduction of *NPF* happen on d4 of tumor induction (Fig. 2a, Fig. 3b), one day prior to the onset of anorexic behavior (Fig. 1h). We therefore asked whether reduced intake for protein-rich food in Yki^{act} male flies (Fig. 4d) is not just the result of anorexia but instead the consequence of an earlier imbalance (e.g., on d4) in dietary choices that worsens the already tumor-compromised state of the animal. To test this, we used the Flypad to conduct a two-choice behavioral assay (yeast vs sugar). When testing control male flies, we observed that their choice for protein-rich food (yeast) over sugar was elevated at dusk compared to dawn (Ext Data Fig. 3d), indicating that macronutrient preference is likely regulated by daily rhythms, similar to overall food intake[49]. Taking advantage of this observation, we assayed d4 Yki^{act} male flies at dusk and discovered that they chose significantly less protein-rich food compared to control (Fig. 4e).

Similarly, when we tested *mef2^{TS} >upd3 + ImpL2* male flies on d1 (an early timepoint with food intake similar to control, Ext. Data Fig. 3e-f), we found that they chose significantly less yeast compared to control (Fig. 4f). These data underscore that the combined increase of

Upd3 and ImpL2 in Yki^{act} male flies on d4 leads to an imbalance in protein-preference. Finally, we tested the impact of NPF signaling in low protein-appetite of Yki^{act} male flies. Interestingly, NPF activation was sufficient to rescue the reduced preference for yeast (Fig. 4g). In addition, NPF activation only from the gut did not rescue the phenotype and further reduced the choice for sugar (Fig. 4g), supporting that dysfunction in NPF signaling from the brain and not the gut is required for reduced preference for protein-rich food. Taken together, we propose that in Yki^{act} male flies at d4 of tumor induction, the combined excess of ImpL2 and Upd3 results in the silencing of NPF neurons in the brain leading to a very early imbalance in protein-rich food preference. Persistent neuronal NPF dysfunction by d5 leads to anorexia and prevents Yki^{act} male flies from meeting their nutritional needs. This subsequently worsens the already tumor-compromised state of the fly and brings on the onset of organ wasting, which is indicated by the reduction in weight by d6 (Fig. 4h).

Our findings in colorectal tumor flies support that very early changes in protein-specific appetites drive the onset of anorexia and the subsequent advent of organ wasting symptoms. Specifically, our work reveals that in Yki^{act} male flies, neuronal NPF/NPY dysfunction caused by the synergy of high Upd3/IL6 and ImpL2/IGFBP is a key regulator of anorexia, protein-appetite imbalance, and early weight loss. Taken together, our data provide evidence that link: i) the increase of IL-6 and IGFBPs to the onset of anorexia prior to organ wasting; ii) NPY dysfunction to early-stage weight loss during CC; iii) early imbalance in protein-specific appetites to CC progression. These findings could help identify early markers of CC in humans and uncover the etiology behind the onset of this lethal syndrome.

References:

1 Ferrer, M. *et al.* Cachexia: A systemic consequence of progressive, unresolved disease. *Cell* 186, 1824-1845, doi:10.1016/j.cell.2023.03.028 (2023).

2 Yeom, E. & Yu, K. Understanding the molecular basis of anorexia and tissue wasting in cancer cachexia. *Exp Mol Med* 54, 426-432, doi:10.1038/s12276-022-00752-w (2022).

3 Argiles, J. M., Busquets, S., Stemmler, B. & Lopez-Soriano, F. J. Cancer cachexia: understanding the molecular basis. *Nat Rev Cancer* 14, 754-762, doi:10.1038/nrc3829 (2014).

4 Kwon, Y. *et al.* Systemic organ wasting induced by localized expression of the secreted insulin/IGF antagonist ImpL2. *Dev Cell* 33, 36-46, doi:10.1016/j.devcel.2015.02.012 (2015).

5 Ding, G. *et al.* Coordination of tumor growth and host wasting by tumor-derived Upd3. *Cell Rep* 36, 109553, doi:10.1016/j.celrep.2021.109553 (2021).

6 Liu, Y., Saavedra, P. & Perrimon, N. Cancer cachexia: lessons from Drosophila. *Dis Model Mech* 15, doi:10.1242/dmm.049298 (2022).

7 Saavedra, P. *et al.* REPTOR and CREBRF encode key regulators of muscle energy metabolism. *Nat Commun* 14, 4943, doi:10.1038/s41467-023-40595-1 (2023).

8 Itskov, P. M. *et al.* Automated monitoring and quantitative analysis of feeding behaviour in Drosophila. *Nat Commun* 5, 4560, doi:10.1038/ncomms5560 (2014).
9 Wang, X. *et al.* IGFBP-3 promotes cachexia-associated lipid loss by suppressing insulin-like growth factor/insulin signaling. *Chin Med J (Engl)* 136, 974-985, doi:10.1097/CM9.0000000000002628 (2023).
10 Huang, X. Y. *et al.* Pancreatic cancer cell-derived IGFBP-3 contributes to muscle wasting. *J Exp Clin Cancer Res* 35, 46, doi:10.1186/s13046-016-0317-z (2016).
11 Sun, Q. *et al.* Area postrema neurons mediate interleukin-6 function in cancer cachexia. *Nat Commun* 15, 4682, doi:10.1038/s41467-024-48971-1 (2024).
12 Ding, G. *et al.* REV-ERB in GABAergic neurons controls diurnal hepatic insulin sensitivity. *Nature* 592, 763-767, doi:10.1038/s41586-021-03358-w (2021).
13 Kim, J. *et al.* Tumor-induced disruption of the blood-brain barrier promotes host death. *Dev Cell* 56, 2712-2721 e2714, doi:10.1016/j.devcel.2021.08.010 (2021).
14 Figueroa-Clarevega, A. & Bilder, D. Malignant Drosophila tumors interrupt insulin signaling to induce cachexia-like wasting. *Dev Cell* 33, 47-55, doi:10.1016/j.devcel.2015.03.001 (2015).
15 Beshel, J., Dubnau, J. & Zhong, Y. A Leptin Analog Locally Produced in the Brain Acts via a Conserved Neural Circuit to Modulate Obesity-Linked Behaviors in Drosophila. *Cell Metab* 25, 208-217, doi:10.1016/j.cmet.2016.12.013 (2017).
16 Wu, Q., Zhang, Y., Xu, J. & Shen, P. Regulation of hunger-driven behaviors by neural ribosomal S6 kinase in Drosophila. *Proc Natl Acad Sci U S A* 102, 13289-13294, doi:10.1073/pnas.0501914102 (2005).
17 Lin, S., Senapati, B. & Tsao, C. H. Neural basis of hunger-driven behaviour in Drosophila. *Open Biol* 9, 180259, doi:10.1098/rsob.180259 (2019).
18 Rajan, A. & Perrimon, N. Drosophila cytokine unpaired 2 regulates physiological homeostasis by remotely controlling insulin secretion. *Cell* 151, 123-137, doi:10.1016/j.cell.2012.08.019 (2012).
19 Ribeiro, C. & Dickson, B. J. Sex peptide receptor and neuronal TOR/S6K signaling modulate nutrient balancing in Drosophila. *Curr Biol* 20, 1000-1005, doi:10.1016/j.cub.2010.03.061 (2010).
20 Sun, J. *et al.* Drosophila FIT is a protein-specific satiety hormone essential for feeding control. *Nat Commun* 8, 14161, doi:10.1038/ncomms14161 (2017).
21 Malita, A. *et al.* A gut-derived hormone suppresses sugar appetite and regulates food choice in Drosophila. *Nat Metab* 4, 1532-1550, doi:10.1038/s42255-022-00672-z (2022).
22 Camus, M. F., Huang, C. C., Reuter, M. & Fowler, K. Dietary choices are influenced by genotype, mating status, and sex in Drosophila melanogaster. *Ecol Evol* 8, 5385-5393, doi:10.1002/ece3.4055 (2018).
23 Hadjieconomou, D. *et al.* Enteric neurons increase maternal food intake during reproduction. *Nature* 587, 455-459, doi:10.1038/s41586-020-2866-8 (2020).
24 Walker, S. J., Corrales-Carvajal, V. M. & Ribeiro, C. Postmating Circuitry Modulates Salt Taste Processing to Increase Reproductive Output in Drosophila. *Curr Biol* 25, 2621-2630, doi:10.1016/j.cub.2015.08.043 (2015).
25 Carvalho, G. B., Kapahi, P., Anderson, D. J. & Benzer, S. Allocrine modulation of feeding behavior by the Sex Peptide of Drosophila. *Curr Biol* 16, 692-696, doi:10.1016/j.cub.2006.02.064 (2006).
26 Sano, H. *et al.* The Nutrient-Responsive Hormone CCHamide-2 Controls Growth by Regulating Insulin-like Peptides in the Brain of Drosophila melanogaster. *PLoS Genet* 11, e1005209, doi:10.1371/journal.pgen.1005209 (2015).
27 Li, S. *et al.* Expression patterns of the Drosophila neuropeptide CCHamide-2 and its receptor may suggest hormonal signaling from the gut to the brain. *PLoS One* 8, e76131, doi:10.1371/journal.pone.0076131 (2013).

28 Ren, G. R. *et al.* CCHamide-2 Is an Orexigenic Brain-Gut Peptide in Drosophila. *PLoS One* 10, e0133017, doi:10.1371/journal.pone.0133017 (2015).
29 Brown, M. R. *et al.* Identification of a Drosophila brain-gut peptide related to the neuropeptide Y family. *Peptides* 20, 1035-1042, doi:10.1016/s0196-9781(99)00097-2 (1999).
30 Yoshinari, Y. *et al.* The sugar-responsive enteroendocrine neuropeptide F regulates lipid metabolism through glucagon-like and insulin-like hormones in Drosophila melanogaster. *Nat Commun* 12, 4818, doi:10.1038/s41467-021-25146-w (2021).
31 Inagaki, H. K., Panse, K. M. & Anderson, D. J. Independent, reciprocal neuromodulatory control of sweet and bitter taste sensitivity during starvation in Drosophila. *Neuron* 84, 806-820, doi:10.1016/j.neuron.2014.09.032 (2014).
32 Hergarden, A. C., Tayler, T. D. & Anderson, D. J. Allatostatin-A neurons inhibit feeding behavior in adult Drosophila. *Proc Natl Acad Sci U S A* 109, 3967-3972, doi:10.1073/pnas.1200778109 (2012).
33 Chung, B. Y. *et al.* Drosophila Neuropeptide F Signaling Independently Regulates Feeding and Sleep-Wake Behavior. *Cell Rep* 19, 2441-2450, doi:10.1016/j.celrep.2017.05.085 (2017).
34 Beshel, J. & Zhong, Y. Graded encoding of food odor value in the Drosophila brain. *J Neurosci* 33, 15693-15704, doi:10.1523/JNEUROSCI.2605-13.2013 (2013).
35 Krashes, M. J., Keene, A. C., Leung, B., Armstrong, J. D. & Waddell, S. Sequential use of mushroom body neuron subsets during drosophila odor memory processing. *Neuron* 53, 103-115, doi:10.1016/j.neuron.2006.11.021 (2007).
36 Landayan, D., Wang, B. P., Zhou, J. & Wolf, F. W. Thirst interneurons that promote water seeking and limit feeding behavior in Drosophila. *Elife* 10, doi:10.7554/eLife.66286 (2021).
37 Yeom, E. *et al.* Tumour-derived Dilp8/INSL3 induces cancer anorexia by regulating feeding neuropeptides via Lgr3/8 in the brain. *Nat Cell Biol* 23, 172-183, doi:10.1038/s41556-020-00628-z (2021).
38 Chance, W. T., Balasubramaniam, A. & Fischer, J. E. Neuropeptide Y and the development of cancer anorexia. *Ann Surg* 221, 579-587; discussion 587-579, doi:10.1097/00000658-199505000-00016 (1995).
39 Meguid, M. M. *et al.* Tumor anorexia: effects on neuropeptide Y and monoamines in paraventricular nucleus. *Peptides* 25, 261-266, doi:10.1016/j.peptides.2004.01.012 (2004).
40 Wahid, I. The role of neuropeptide y in cancer-associated anorexia and its correlation with interleukin-1 beta. *Annals of Oncology* 28, doi:10.1093/annonc/mdx676.010 (2017).
41 Jatoi, A., Loprinzi, C. L., Sloan, J. A., Klee, G. G. & Windschitl, H. E. Neuropeptide Y, leptin, and cholecystokinin 8 in patients with advanced cancer and anorexia: a North Central Cancer Treatment Group exploratory investigation. *Cancer* 92, 629-633, doi:10.1002/1097-0142(20010801)92:3<629::aid-cncr1363>3.0.co;2-m (2001).
42 Ragni, M., Fornelli, C., Nisoli, E. & Penna, F. Amino Acids in Cancer and Cachexia: An Integrated View. *Cancers (Basel)* 14, doi:10.3390/cancers14225691 (2022).
43 Mayers, J. R. *et al.* Elevation of circulating branched-chain amino acids is an early event in human pancreatic adenocarcinoma development. *Nat Med* 20, 1193-1198, doi:10.1038/nm.3686 (2014).
44 Koyama, T., Texada, M. J., Halberg, K. A. & Rewitz, K. Metabolism and growth adaptation to environmental conditions in Drosophila. *Cell Mol Life Sci* 77, 4523-4551, doi:10.1007/s00018-020-03547-2 (2020).
45 Itskov, P. M. & Ribeiro, C. The dilemmas of the gourmet fly: the molecular and neuronal mechanisms of feeding and nutrient decision making in Drosophila. *Front Neurosci* 7, 12, doi:10.3389/fnins.2013.00012 (2013).

46 Augustine, V., Lee, S. & Oka, Y. Neural Control and Modulation of Thirst, Sodium Appetite, and Hunger. *Cell* 180, 25-32, doi:10.1016/j.cell.2019.11.040 (2020).
47 Durham, W. J., Dillon, E. L. & Sheffield-Moore, M. Inflammatory burden and amino acid metabolism in cancer cachexia. *Curr Opin Clin Nutr Metab Care* 12, 72-77, doi:10.1097/MCO.0b013e32831cef61 (2009).
48 Hutton, J. L. *et al.* Dietary patterns in patients with advanced cancer: implications for anorexia-cachexia therapy. *Am J Clin Nutr* 84, 1163-1170, doi:10.1093/ajcn/84.5.1163 (2006).
49 Xu, K., Zheng, X. & Sehgal, A. Regulation of feeding and metabolism by neuronal and peripheral clocks in Drosophila. *Cell Metab* 8, 289-300, doi:10.1016/j.cmet.2008.09.006 (2008).

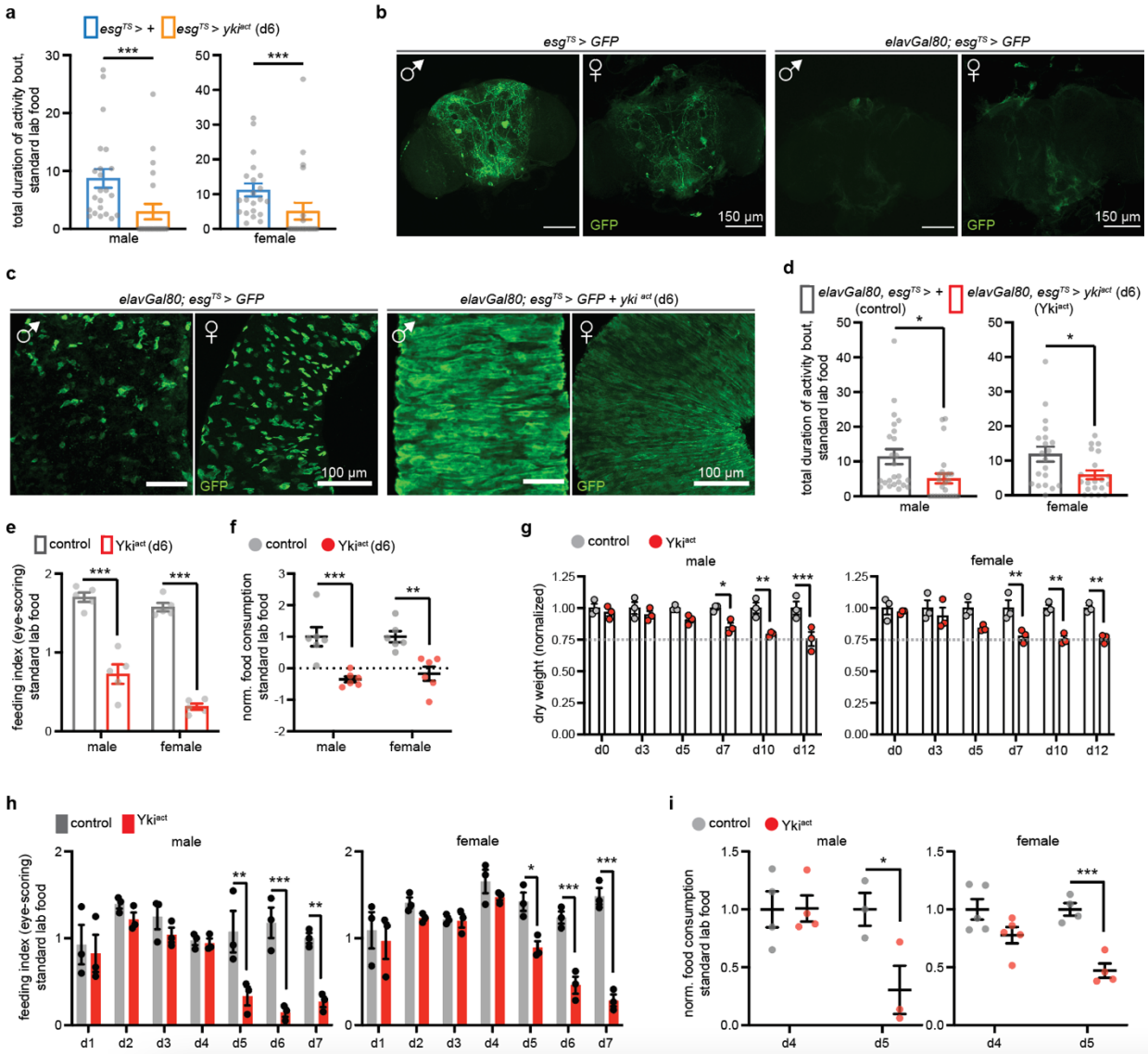

Figure 1: Colorectal-specific Yki-tumors (Yki^{act}) cause anorexia prior to organ wasting. **a.** Flypad-based behavioral feeding assay with standard lab food. We tested control (*esg^{TS}*>+, blue square) and flies with colorectal tumor (*esg^{TS}*>*yki^{act}*, orange square) induced for 6 days. Graphs show the total duration of activity bout (total duration an individual fly touches the food, grey dot) in male (left) and female (right) flies. Male: n= 22 flies per genotype. Female: n=21 flies per genotype. p-values were obtained with Mann-Whitney test. **b.** Confocal images of male and female brains from flies with the *escargot* Gal4 driver conditionally expressing GFP (*esg^{TS}*>*GFP*) and from flies co-expressing the neuronal elavGal80 inhibitor (*elavGal80;esg^{TS}*>*GFP*) for 6 days. anti-GFP (green). scale bar: 150µm. **c.** Confocal images of guts in male and female of control (*elavGal80;esg^{TS}*>*GFP*) and of flies with Yki activation in the gut for 6 days without expression in the brain (*elavGal80;esg^{TS}*>*GFP +yki^{act}*). Anti-GFP: green.

scale bar: 100μm. **d.** Flypad-based behavioral feeding assay with lab food. We tested control (*elavGal80;esg*^{TS}>+, grey square) and flies with colorectal-specific Yki induction for 6 days without expression in the brain (*elavGal80;esg*^{TS}>*yki*^{act}, referred hereafter as Yki^{act}, red square). Graphs show the total duration of activity bout (grey dot) in male (left) and female (right) flies. Male: n= 24 flies per genotype. Female: n=20 flies per genotype. p-values were obtained with Mann-Whitney test. **e.** Blue-dye based feeding assay testing lab food intake of control (*elavGal80;esg*^{TS}>+, grey square) and Yki^{act} (*elavGal80;esg*^{TS}>*yki*^{act} , red square) flies on d6. Graph shows the feeding index based on eye-scoring of males (left) and females (right) per genotype. n= 5 biological samples per genotype in male and female. p-values were obtained with two-way Anova using Sidak's multiple comparisons test. **f.** Blue-dye based feeding assay testing the lab food intake of control (*elavGal80;esg*^{TS}> +, grey circle) and Yki^{act} (*elavGal80;esg*^{TS}>*yki*^{act}, red circle) flies on d6. Graph shows food consumption measured via color spectrophotometry of homogenized samples and normalized to control in male and female. n= 6 biological samples per genotype in male and female. p-values were obtained with two-way Anova using Sidak's multiple comparisons test. **g.** Graphs show dry weight of control (*elavGal80;esg*^{TS}>+, grey circle) and Yki^{act} (*elavGal80;esg*^{TS}>*yki*^{act}, red circle) flies from d0 (no tumor induction) to d12 in male (left) and female (right). n= 3 biological samples per genotype per timepoint. Dry weight is normalized to control in male and female. p-values were obtained with two-way Anova using Sidak multiple comparisons test. **h.** Graphs show the feeding index from blue-dye eye-scoring assay comparing lab food intake of control (*elavGal80;esg*^{TS}>+, grey) and Yki^{act} (*elavGal80;esg*^{TS}>*yki*^{act}, red) flies from d1 to d7 in male (left) and female (right). n= 3 biological samples per genotype per timepoint. p-values were obtained with two-way Anova using Sidak's multiple comparisons test. **i.** Graphs show food consumption measured via color spectrophotometry of control (*elavGal80;esg*^{TS}>+, grey) and Yki^{act} (*elavGal80;esg*^{TS}>*yki*^{act} , red) homogenized flies on d4 and d5 in male (left) and female (right). Values are normalized to control per timepoint. Male: n=4 biological samples per genotype on d4; n=3 biological samples per genotype on d5. Female: n=5 biological samples per genotype on d4; n=4 biological samples per genotype on d5. p-values were obtained with two-way Anova using Sidak's multiple comparisons test. Each experiment was repeated 2-4 times. *: 0.05>p>0.01, **: 0.01<p<0.001, ***: p<0.001. Mean ± s.e.m.

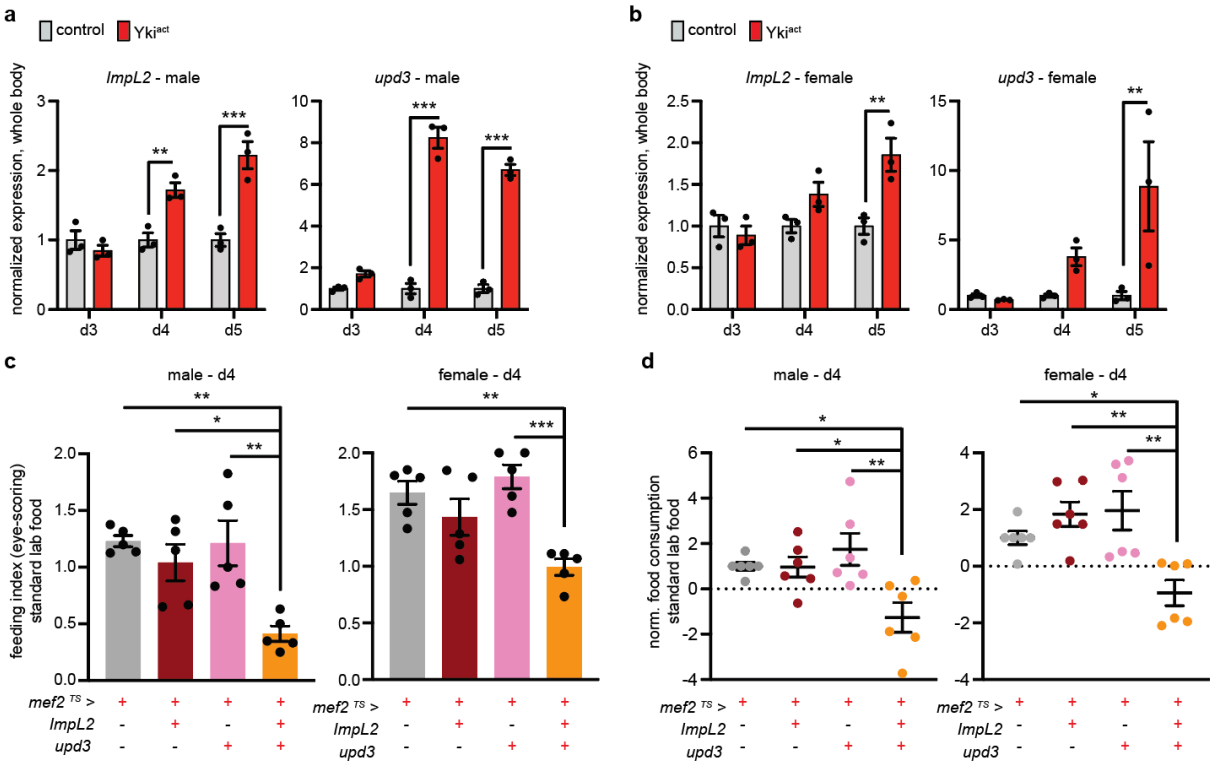

Figure 2: Combined ImpL2 and Upd3 increase leads to anorexia-like behavior.

a-b. Expression levels of conserved neoplastic factors *ImpL2* and *upd3* from whole body of control (*elavGal80;esg*^{TS}>+, grey square) and Yki^{act} (*elavGal80;esg*^{TS}>*yki*^{act} , red square) flies on d3, d4 and d5 of tumor induction in male (a) and female (b). n=3 biological samples per genotype per timepoint. Normalized to control per timepoint. p-values were obtained with two-way Anova using Sidak's multiple comparisons test. **c.** Blue-dye based feeding assay testing lab food intake of control (*mef*^{TS}>+), of flies with *Impl2* (*mef*^{TS}>*ImpL2,* burgundy*)*, or with *upd3* (*mef*^{TS}>*upd3,* magenta), or with *Impl2* and *upd3* (*mef*^{TS}>*ImpL2+upd3,* orange) overexpressed from the muscle for 4 days. Graphs show the feeding index based on eye-scoring in male (left) and in female (right). n= 5 biological samples per genotype. p-values were obtained with one-way Anova using Tukey's multiple comparisons test. **d.** Graphs show food consumption measured via color spectrophotometry of control (*mef*^{TS}>+), of flies with *Impl2* (*mef*^{TS}>*ImpL2,* burgundy), with *upd3* (*mef*^{TS}>*upd3,* magenta), or with *Impl2* and *upd3* (*mef*^{TS}>*ImpL2+upd3,* orange) overexpressed from the muscle for 4 days. Left: male, right: female. Values are normalized to control. n= 6 biological samples per genotype. p-values were obtained with one-way Anova using Tukey's multiple comparisons test. Each experiment was repeated 2-3 times. *: 0.05>p>0.01, **: 0.01<p<0.001, ***: p<0.001. Mean ± s.e.m.

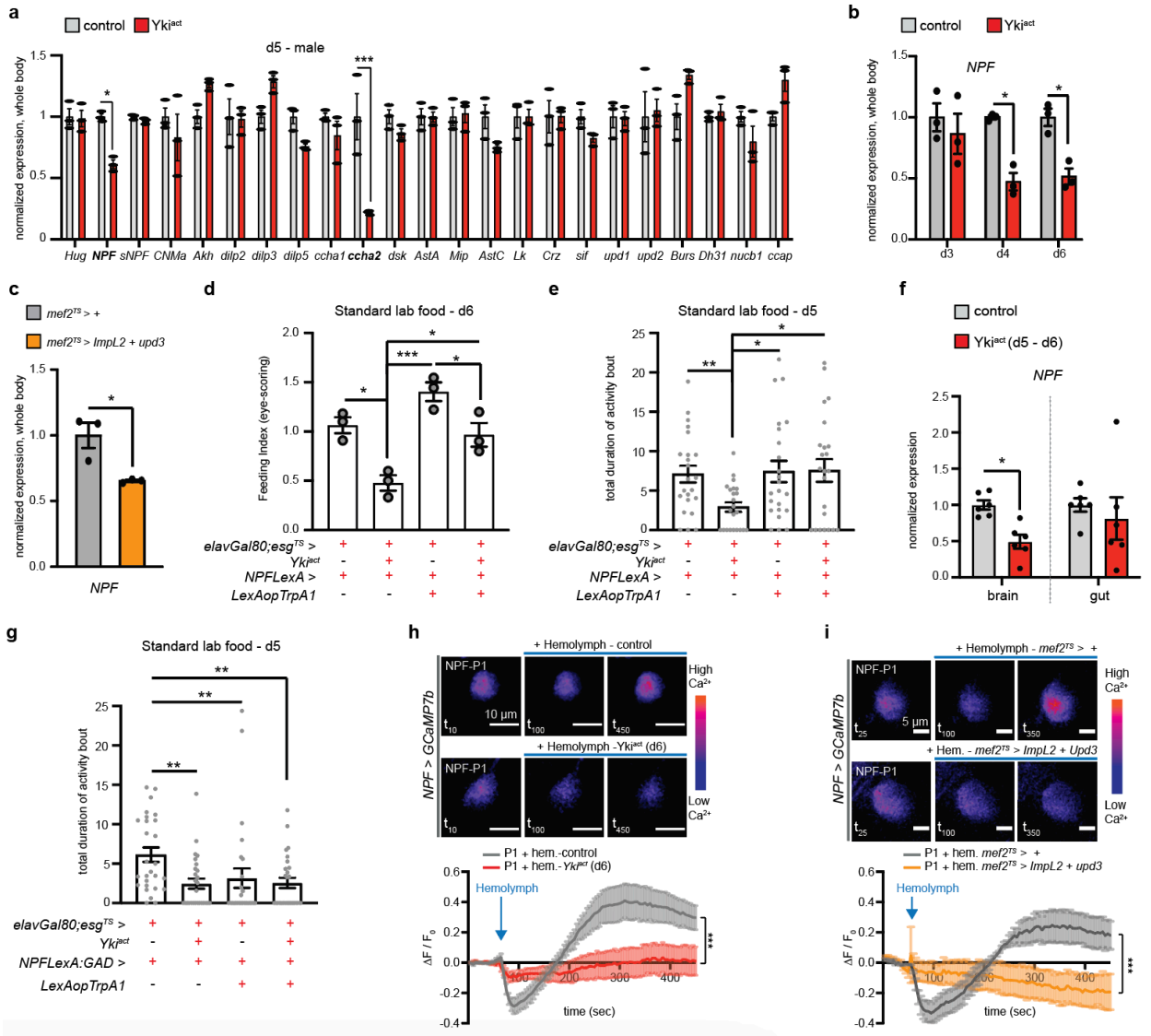

Figure 3: Early NPF dysfunction in the brain due to ImpL2 and Upd3 increase drives anorexia in Yki^{act} male flies. a. Expression levels of feeding-related signals from whole body of male control (*elavGal80;esg^{TS}*>+, grey square) and Yki^{act} (*elavGal80;esg^{TS}>yki^{act}*, red square) male flies on d5 of tumor induction. Normalized to control. n=3 biological samples per genotype. p-values were obtained with two-way Anova using Sidak's multiple comparisons test. *Hug*: *Huggin*, *NPF*: *Neuropeptide F*, *sNPF*: *short Neuropeptide F*, *CNMa*: *CNMamide*, *Akh*: *Adipokinetic hormone*, *dilp2*: *Insulin-like peptide 2*, *dilp3*: *Insulin-like peptide 3*, *dilp5*: *Insulin-like peptide 5*, *ccha1: CCHamide*, *ccha2: CCHamide2*, *dsk: drosulfakinin*, *AstA: Allatostatin A*, *mip: myoinhibitory*, *AstC: Allatostatin C*, *Lk: Leucokinin*, *Crz: Corazonin*, *sif: SIFamide*, *upd1: unpaired1*, *upd2: unpaired2*, *Burs: Bursicon*, *Dh31: diuretic hormone 31*, *nucb1*: *nucleobindin-1*, *ccap: Crustacean cardioactive peptide*. **b.** Expression levels of *NPF* from whole body of control

(*elavGal80;esg*^{TS}>+, grey square) and Yki^{act} (*elavGal80;esg*^{TS}>*yki*^{act} , red square) male flies on d3, d4 and d6 of tumor induction. Normalized to control per timepoint. n=3 biological samples per genotype and timepoint. p-values were obtained with two-way Anova using Sidak's multiple comparisons test. **c.** Expression levels of *NPF* from whole body of male control (*mef2*^{TS}>+, grey square) and of male flies with *ImpL2* and *upd3* overexpressed from the muscle for 4 days (*mef2*^{TS}> *ImpL2+upd3*, orange square). Normalized to control. n=3 biological samples per genotype. p-values were obtained with unpaired t-test. **d.** Blue-dye based feeding assay testing lab food intake of control (*elavGal80;esg*^{TS}*/+;NPFLexA/+*), Yki^{act} (*elavGal80;esg*^{TS}>*yki*^{act} + *NPFLexA*>+), of male flies with increased NPF signaling (*NPFLexA>LexAopTrpA1* + *elavGal80;esg*^{TS}>+) and flies with increased NPF signaling together with Yki-tumor growth (*NPFLexA>LexAopTrpA1* + *elavGal80;esg*^{TS}>*yki*^{act}). Graph shows the feeding index based on eye-scoring of male flies on d6. n= 3 biological samples per genotype. p-values were obtained with one-way Anova using Tukey's multiple comparisons test. **e.** Flypad-based behavioral feeding assay with lab food. Graph shows the total duration of activity bout on d5 of male flies as in (d). n=23 flies per genotype. p-values were obtained with Kruskal Wallis uncorrected Dunn's test. **f.** Expression levels of *NPF* from brain and gut of control (*elavGal80;esg*^{TS}>+, grey square) and Yki^{act} (*elavGal80;esg*^{TS}>*yki*^{act}, red square) male flies on d5 and d6. n= 6 biological samples per tissue and genotype. Normalized to control per tissue. p-values were obtained with two-way Anova using Sidak's multiple comparisons test. **g.** Flypad-based behavioral feeding assay with lab food testing control (*elavGal80;esg*^{TS}*/+;NPFLexA:GAD/+*), Yki^{act} flies (*elavGal80;esg*^{TS}>*yki*^{act} + *NPFLexA:GAD*>+), flies with increased NPF signaling from the gut (*NPFLexA:GAD>LexAopTrpA1* + *elavGal80;esg*^{TS}>+) and flies with increased NPF signaling from the gut together with Yki-tumor growth (*NPFLexA:GAD>LexAopTrpA1* + *elavGal80;esg*^{TS}>*yki*^{act}). Graph shows the total duration of activity bout on d5 of male flies. n= 27 flies per genotype. p-values were obtained with Kruskal Wallis uncorrected Dunn's test. **h.** Color-coded sequential frames of NPF-P1 neuron from brains of male flies with Ca^{2+} indicator GCAMP7b expressed in NPF neurons (*NPF>GCAMP7b*) before (t_{10}) and after (t_{100}), (t_{450}) hemolymph addition. Videos S1-S2. Accompanying graph: average relative fluorescence intensity ($\Delta F/F_0$) per frame (5 sec/frame). Control hemolymph: from *elavGal80;esg*^{TS}>+ male flies (grey line). Yki^{act} hemolymph: from *elavGal80;esg*^{TS}>*yki*^{act} male flies on d6 (red line).n= 5 neurons per condition. p-values were obtained with two-way Anova using Tukeys's multiple comparisons test. Individual $\Delta F/F_0$ shown on Ext. Data Fig. 2d. scale bar: 10μm. **i.** Color-coded sequential frames of NPF-P1 neuron from brains of male flies with Ca^{2+} indicator GCAMP7b expressed in NPF neurons (*NPF>GCAMP7b*) before (t_{25}) and after (t_{100}), (t_{350}) hemolymph

addition. Videos S3-S4. Accompanying graph: average relative fluorescence intensity ($\Delta F/F_0$) per frame (5 sec/frame). Control hemolymph: from *mef2*^{TS}>+ male flies (grey line). *mef2*^{TS}>*ImpL2*+*upd3* hemolymph: from *mef2*^{TS}>*ImpL2*+*upd3* male flies on d4 (orange line). n= 3 neurons per condition. p-values were obtained with two-way Anova using Tukeys's multiple comparisons test. Individual $\Delta F/F_0$ shown on Ext. Data Fig. 2e. scale bar: 5μm. Each experiment was repeated 2-3 times. *: 0.05>p>0.01, **: 0.01<p<0.001, ***: p<0.001. Mean ± s.e.m.

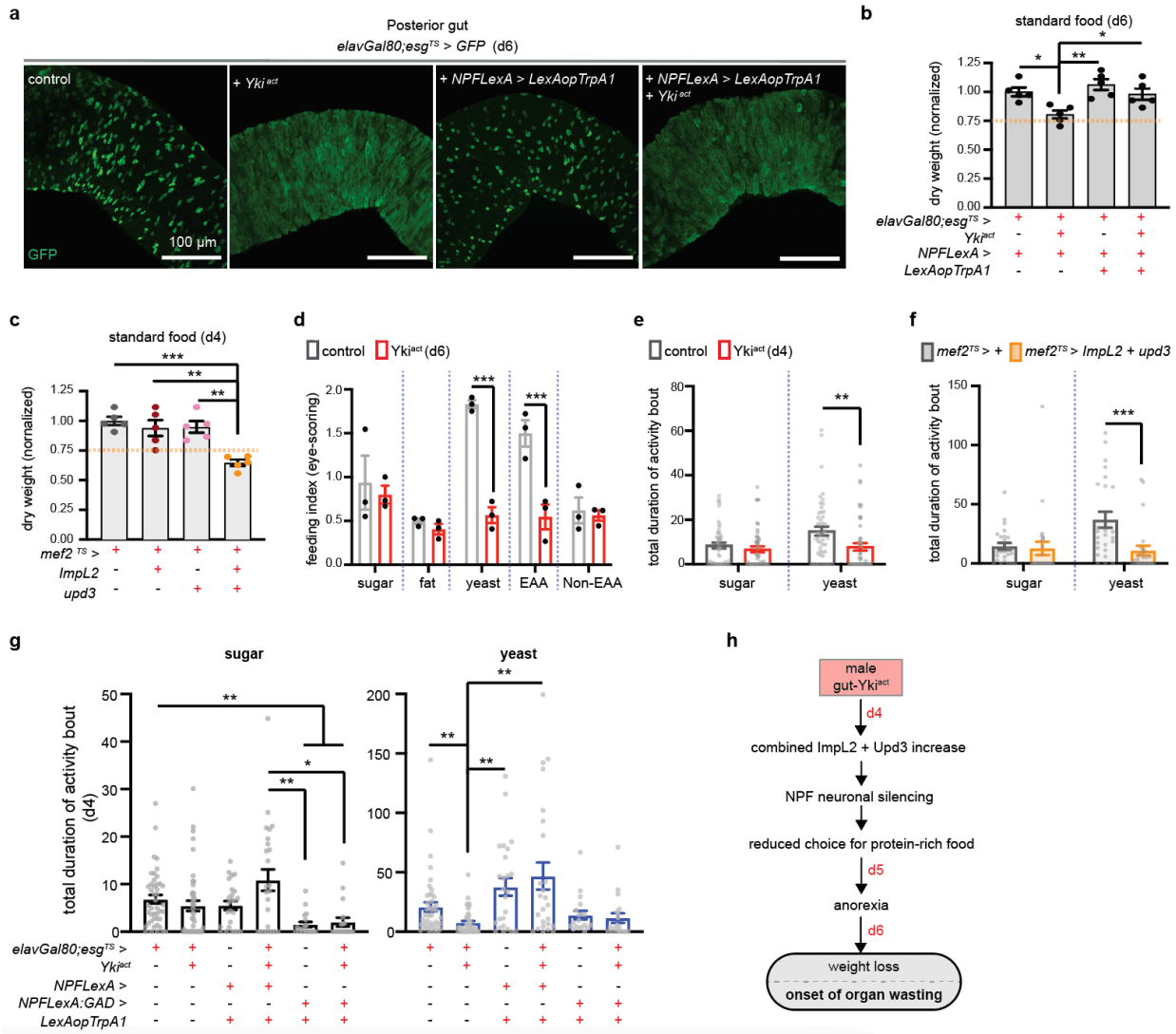

Figure 4: NPF activation in male Yki^{act} flies rescues early weight loss and protein-rich food preferences. **a.** Confocal images of male guts with GFP expression in progenitor cells on d6 of control (*elavGal80;esg^{TS}*>GFP), Yki^{act} (*elavGal80;esg^{TS}>GFP+ yki^{act}*), flies with increased NPF signaling (*elavGal80;esg^{TS}>GFP + NPFLexA:LexAopTrpA1*) and flies with increased NPF signaling together with Yki-tumor growth (*NPFLexA: LexAopTrpA1 + elavGal80;esg^{TS}>GFP + yki^{act}*). Anti-GFP: green. scale bar: 100µm. **b.** Graph shows dry weight on d6 of control (*elavGal80;esg^{TS}/+; NPFLexA/+*), Yki^{act} flies(*elavGal80;esg^{TS}> yki^{act} + NPFLexA>+*), flies with increased NPF signaling (*NPFLexA>LexAopTrpA1 + elavGal80;esg^{TS}>+*) and flies with increased NPF signaling together with Yki-tumor growth (*NPFLexA>LexAopTrpA1 + elavGal80;esg^{TS}>yki^{act}*). n= 5 biological samples per genotype. Normalized to control. p-values were obtained with one-way Anova using Tukey's multiple comparisons test. **c.** Graph showing dry weight of control (*mef2^{TS}>+,* grey circle), of male flies with ImpL2 (*mef2^{TS}>ImpL2,* burgundy

circle), with Upd3 (*mef2^{TS}>upd3,* magenta circle), with ImpL2 and Upd3 (*mef2^{TS}>ImpL2+upd3,* orange circle) increased from the muscle for 4 days. n= 5 biological samples per genotype. Normalized to control. p-values were obtained with one-way Anova using Tukey's multiple comparisons test. **d.** Blue-dye based feeding assay testing intake using different foods. Graph shows feeding index based on eye scoring from control (*elavGal80;esg^{TS}*>+, grey square) and Yki^{act} (*elavGal80;esg^{TS}>yki^{act}*, red square) male flies on d6. n= 3 biological samples per genotype and diet. p-values were obtained with two-way Anova using Sidak's multiple comparisons test. yeast: protein-rich food. EAA: food rich with essential amino acids. Non-EAA: food rich with non-essential amino acids. **e.** Flypad-based sugar vs yeast two choice-assay of control (*elavGal80;esg^{TS}*>+, grey square) and Yki^{act} (*elavGal80;esg^{TS}>yki^{act}*, red square) male flies on d4 at dusk. Graph shows total duration of activity bout for sugar (left) and yeast (right). n= 48 flies per genotype. p-values were obtained with Kruskal Wallis Dunn's multiple comparisons test. **f.** Flypad-based sugar vs yeast two choice-assay of control (*mef2^{TS}*>+, grey square) and male flies with *ImpL2* and *upd3* overexpressed from the muscle for ~18hrs (d1) at dusk (*mef2^{TS}>ImpL2+upd3*, orange square). Graph shows total duration of activity bout for sugar (left) and yeast (right). n= 25 flies per genotype. p-values were obtained with Kruskal Wallis Dunn's multiple comparisons test. **g.** Flypad-based sugar vs yeast two choice-assay of male flies on d4 at dusk. Graphs show total duration of activity bout for sugar (left, black) and yeast (right, blue) from control (*elavGal80;esg^{TS}*>+, n= 44 flies), Yki^{act} flies (*elavGal80;esg^{TS}yki^{act}*, n= 44 flies) and flies with increased NPF signaling (*NPFLexA>LexAopTrpA1* + *elavGal80;esg^{TS}*>+, n= 25 flies), increased NPF signaling together with Yki-tumor growth (*NPFLexA>LexAopTrpA1* + *elavGal80;esg^{TS}>yki^{act}*, n= 25 flies), increased NPF signaling from the gut (*NPFLexA:GAD>LexAopTrpA1* + *elavGal80;esg^{TS}*>+, n= 19 flies), increased NPF signaling from the gut together with Yki-tumor growth (*NPFLexA:GAD>LexAopTrpA1* + *elavGal80;esg^{TS}>yki^{act}* , n= 19 flies). p-values were obtained with Kruskal Wallis Dunn's multiple comparisons test. **h.** Model. In Yki^{act} male flies the combined excess of ImpL2 and Upd3 on d4 silences NPF neurons in the brain causing low preference for protein-rich food. On d5 NPF neuronal dysfunction becomes anorexia specific to protein-rich food and by d6 this malnutrition drives weight loss. Each experiment was repeated 2-4 times. *: 0.05>p>0.01, **: 0.01<p<0.001, ***: p<0.001. Mean $\pm$ s.e.m.

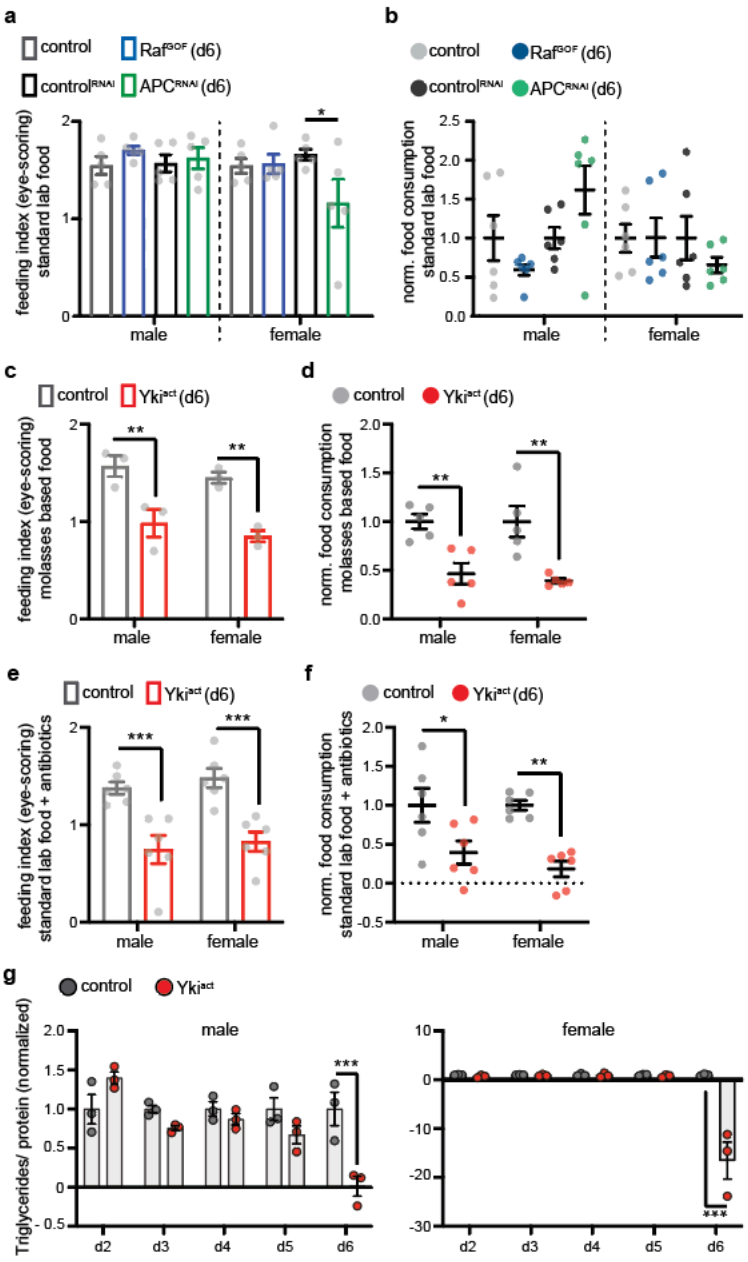

Ext. Data Fig. 1: Tumor-derived anorexia is linked to organ wasting. a. Blue-dye based feeding assay testing lab food intake of control (*elavGal80;esg*^{TS}>+, grey square), Raf^{GOF} (colorectal-specific induction of *Raf* oncogene, *elavGal80;esg*^{TS}>*Raf*^{GOF}, blue square), control^{RNAi} (*elavGal80;esg*^{TS}>*Luciferase*^{RNAi}, black square), APC^{RNAi} (colorectal-specific reduction of *APC* tumor suppressor, *elavGal80;esg*^{TS}>*APC*^{RNAi}, green square). Graph shows the feeding index based on eye-scoring of males (left) and females (right) per genotype on d6. n= 5 biological samples per genotype in male and female. p-values were obtained with two-way Anova using Tukey's multiple comparisons test. **b.** Graph shows food consumption measured

via color spectrophotometry in homogenized flies similar to (a). control: grey circle, Raf^{GOF}: blue circle, $control^{RNAi}$: black circle, APC^{RNAi}: green circle. Left: male, right: female. Normalized to each control. n= 6 biological samples per genotype in male and female. p-values were obtained with two-way Anova using Tukey's multiple comparisons test. **c.** Blue-dye based feeding assay with molasses-based food. control: *elavGal80;esg*^{TS}>+ (grey square). Yki^{act} : *elavGal80;esg*^{TS}>*yki*^{act} (red square). Graph shows the feeding index based on eye-scoring of males (left) and females (right) per genotype on d6. n= 3 biological samples per genotype in male and female. p-values were obtained with two-way Anova using Sidak's multiple comparisons test. **d.** Food consumption measured via color spectrophotometry using molasses-based food. Flies similar to (c). control: grey circle. Yki^{act}: red circle. Graph shows normalized food intake on d6 in male (left) and female (right). Normalized to control. n= 5 biological samples per genotype in male and female. p-values were obtained with two-way Anova using Sidak's multiple comparisons test. **e.** Blue-dye based feeding assay using lab food with antibiotics. control: *elavGal80; esg*^{TS}>+ (grey square). Yki^{act}: *elavGal80;esg*^{TS}>*yki*^{act} (red square). Graph shows the feeding index based on eye-scoring of males (left) and females (right) per genotype on d6. n= 6 biological samples per genotype in male and female. p-values were obtained with two-way Anova using Sidak's multiple comparisons test. **f.** Food consumption measured via color spectrophotometry using lab food with antibiotics. Flies similar to (e). control: grey circle. Yki^{act} : red circle. Graph normalized food intake on d6 in male (left) and female (right). Normalized to control. n= 6 biological samples per genotype in male and female. p-values were obtained with two-way Anova using Sidak's multiple comparisons test. **g.** Metabolic assay testing the levels of triglycerides from d2 to d6 on control (*elavGal80; esg*^{TS}>+, grey circle) and Yki^{act} (*elavGal80;esg*^{TS}>*yki*^{act} (red circle) flies. Normalized per day to control. Graphs show triglyceride over protein levels on male (left) and female (right) flies. n=3 biological samples per genotype in male and female. p-values were obtained with two-way Anova using Sidak's multiple comparisons test. Each experiment was repeated 2-3 times. *: $0.05>p>0.01$, **: $0.01<p<0.001$, ***: $p<0.001$. Mean $\pm$ s.e.m.

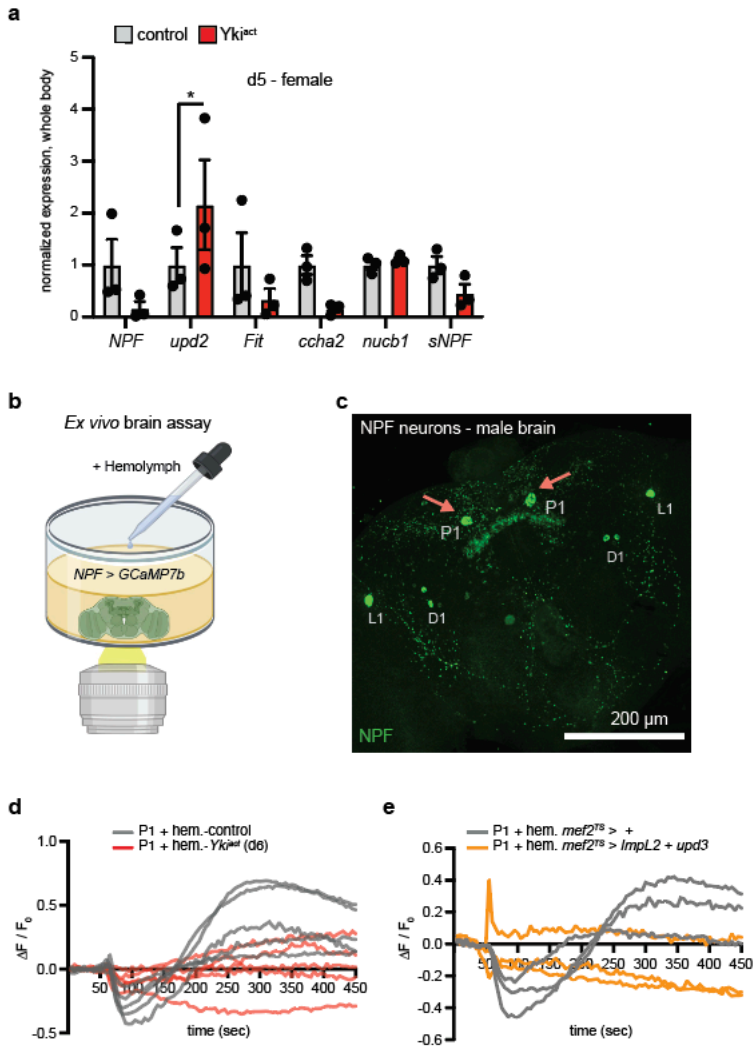

Ext. Data Fig. 2: NPF neurons are silenced by ImpL2 and Upd3 in Yki^{act} male flies. a. Expression levels of feeding-related signals from whole body of female control (*elavGal80; esg^{TS}*>+, grey square) and Yki^{act} (*elavGal80;esg^{TS}>yki^{act}*, red square) female flies on d5 of tumor induction. Normalized to control. n=3 biological samples per genotype. p-values were obtained with two-way Anova (uncorrected Fisher's test). *NPF*: *Neuropeptide F*, *upd2: unpaired2, Fit: Female-specific independent of transformer, ccha2: CCHamide2, nucb1*: *nucleobindin-1, sNPF*: *short Neuropeptide F*. **b.** Illustration showing *ex vivo* brain live-imaging assay that tests the activity of NPF neurons after hemolymph addition. Brains from male flies express the Ca^{2+} indicator GCaMP7b in NPF neurons (*NPF>GCAMP7b*). **c.** Confocal image of a brain from male control (*elavGal80; esg^{TS}*>+) stained with anti-NPF (green). red arrows: dorsal median NPF-P1 neurons that were used for imaging. L1: NPF neurons that are part of the clock network. D1: male specific NPF neurons. **d.** Relative fluorescence intensity ($\Delta F/F_0$) per frame (5 seconds per frame) and per genotype of individual NPF-P1 neurons as described in Fig. 3h. **e.** Relative

fluorescence intensity ($\Delta F/F_0$) per frame (5 seconds per frame) and per genotype of individual NPF-P1 neurons as described in Fig. 3i. Illustration was designed with Biorender.

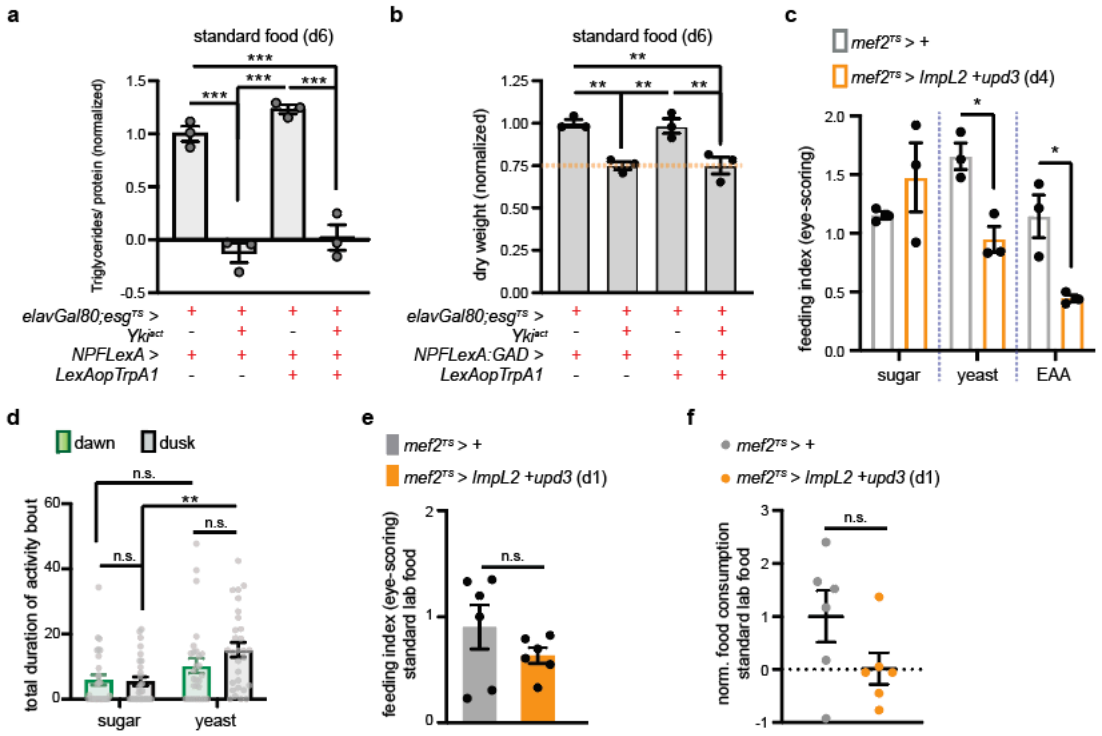

Ext. Data Fig. 3: NPF activation under colorectal Yki-tumor growth. a. Metabolic assay testing the levels of triglycerides from control (*elavGal80;esg^{TS}/+;NPFLexA/+*), Yki^{act} (*elavGal80;esg^{TS}>yki^{act} + NPFLexA>+*), flies with increased NPF signaling (*NPFLexA>LexAopTrpA1 + elavGal80;esg^{TS}>+*) and flies with increased NPF signaling together with Yki-tumor growth (*NPFLexA>LexAopTrpA1 +elavGal80;esg^{TS}>yki^{act}*). Graph shows triglyceride over protein levels on male d6 flies. n=3 biological samples per genotype. Normalized to control. p-values were obtained with one-way Anova using Tukey's multiple comparisons test. **b.** Graph shows dry weight on d6 from male control (*elavGal80;esg^{TS}/+; NPFLexA:GAD/+*), Yki^{act} flies (*elavGal80;esg^{TS}>yki^{act} + NPFLexA:GAD>+*), male flies with increased NPF signaling from the gut (*NPFLexA>LexAopTrpA1 + elavGal80;esg^{TS}>+*) and flies with increased NPF signaling from the gut together with Yki-tumor growth (*NPFLexA>LexAopTrpA1 + elavGal80;esg^{TS}>yki^{act}*). n= 3 biological samples per genotype. Normalized to control. p-values were obtained with one-way Anova using Tukey's multiple comparisons test. **c.** Blue-dye based feeding assay testing intake using sugar-rich, protein-rich (yeast) and essential-amino acid (EAA)-rich food. Graph shows feeding index based on eye scoring from control (*mef2^{TS}>+*, grey square) and male flies with ImpL2 and Upd3 overexpressed from the muscle for 4 days (*mef2^{TS}>ImpL2+upd3*, orange square) n= 3 biological samples per genotype and diet. p-values were obtained with two-way Anova using Sidak's

multiple comparisons test. **d.** Flypad-based sugar vs yeast two choice-assay of control (*elavGal80;esg*^{TS}>+) male flies at dawn (ZT0-ZT2, green) and dusk (ZT10-ZT12, black) on d4. Graph shows total duration of activity bout for sugar (left) and yeast (right). n= 29 flies per genotype. p-values were obtained with Kruskal Wallis Dunn's multiple comparisons test. **e-f.** Blue-dye based feeding assays testing lab food intake of control (*mef*^{TS}>+) and of male flies with *Impl2* and *upd3* (*mef*^{TS}>*ImpL2+upd3,* orange) overexpressed from the muscle for ~18hrs (d1). Graph in (e) shows the feeding index based on eye-scoring. Graph in (f) shows food consumption based on color spectrophotometry of homogenized samples. n= 6 biological samples per genotype and per assay. p-values were obtained with unpaired t-test. Each experiment was repeated 2-4 times. n.s: non-significant. *: 0.05>p>0.01, **: 0.01<p<0.001, ***: p<0.001. Mean $\pm$ s.e.m